

NUMERICAL SIMULATION OF POOL BOILING: THE EFFECTS OF INITIAL THERMAL BOUNDARY LAYER, CONTACT ANGLE AND WALL SUPERHEAT

Anastasios Georgoulas * ^{1,2}, anastasios.georgoulas@unibg.com
Marco Marengo ^{1,2}, M.Marengo@brighton.ac.uk

¹ Dept. of Engineering and Applied Sciences, University of Bergamo, Viale Marconi 5, 24044 Dalmine, Italy
² School of Computing, Engineering and Mathematics, University of Brighton, Lewes Road, BN2 4GJ Brighton, UK

ABSTRACT

Boiling heat transfer has been a subject of extensive investigation during the last decades. Since the sub-processes in nucleate boiling, involve quite complex physics, the development of comprehensive correlations and/or models has not been possible so far. However, more recently, numerical simulations of the boiling process have proven to be capable of reliably predicting bubble dynamics and heat transfer characteristics. In the present paper, heat transfer and phase-change are coupled with a previously improved and validated Volume Of Fluid (VOF) model for adiabatic bubble dynamics. The model is initially verified with an existing analytical solution for cases of evaporating bubble growth in a superheated liquid domain. Moreover, the predictions of the proposed model regarding the bubble detachment characteristics are also validated against available experimental data on pool boiling of refrigerants. The validated and optimised version of the model is further applied for the conduction of a wide range of parametric numerical simulations, identifying the effects of the initial thermal boundary layer thickness, the contact angle between the liquid/vapour interface and the heated plate, as well as the plate superheat, on the bubble detachment characteristics. It is found that the bubble growth and detachment characteristics are highly sensitive to the initially developed thermal boundary layer thickness, following a linear relationship. This has a strong implication on the experimental activities, since in many cases it is not clear at which time the initial measurements of the pool boiling characteristics have been carried out with respect to the time scale to reach the quasi steady-state condition of the thermal boundary layer, linked to the natural convection. As for the imposed contact angle effect, a threshold value is identified below which, the effect on the bubble detachment characteristics is minimal while above this value the influence is quite significant. Moreover, the bubble detachment characteristics follow an exponential increase with the corresponding increase in the superheat of the heated plate.

INTRODUCTION

Boiling heat transfer has been a subject of extensive investigation during the last decades since it constitutes one of the most effective ways to dissipate high heat fluxes, due to the associated high heat transfer coefficients. Therefore, boiling heat transfer is of great interest in a wide range of engineering fields such as, power generation, refrigeration and cooling of electronic devices. Since the underlying sub-processes in nucleate boiling, involve quite complex physics, the development of comprehensive correlations and/or models has not been possible so far. However, with the growing computing capabilities and available computational resources as well as with the rapid development of modern numerical methods for the simulation of multiphase-phase flows, the numerical simulation of boiling heat transfer has become possible, for a wide range of applications as well as spatial and temporal scales. Therefore, the numerical simulation of boiling heat transfer in the near future could be established as an excellent tool that in conjunction with highly resolved laboratory experiments could provide significant insight regarding the underlying physical mechanisms.

One of the most promising numerical tools for the analysis of boiling heat transfer is the use of Computational Fluid Dynamics (CFD) codes. In the recent years, the use of CFD codes has been extended to the analysis of three-dimensional, multi-phase flows, aiming to overcome the weakness of 1D numerical models. Typically, up to present, there are two main branches in the literature for the numerical investigation of boiling heat transfer by the use of CFD.

In the first branch, most of the existing open-source, in-house, and especially commercial CFD codes have adopted an Eulerian multiphase flow approach, based on a two-fluid model. For the case of boiling flows, where heat is transferred into the fluid from a heated wall at rates that boiling happens and vapour is generated, additional source terms describing the physics of these processes at the heated wall, have to be included in the governing equations. For this purpose these global multi-phase CFD models are usually coupled with appropriate wall boiling sub-models, like the most widely used wall-partitioning model of Kurul and Podowski (1990). Some representative and relatively recent numerical investigations in this branch are the works by Lopez-de-Bertodano et al. (2010), Yun et al. (2013) and Krepper et al. (2013). However, such wall boiling sub-models require additional closure relationships that predict the bubble departure characteristics and the density of the active nucleation sizes that incorporate a lot of model constants, the value of which can be found only for specific flow conditions and working fluids. Recently, in the works of Prabhudharwadkar et al. (2014) and Cheung et al. (2014), the performance of a wide combination range of such existing closure relationships is examined through comparison with a wide range of experimental data. It is stated that not one single combination of empirical correlations has shown the propensity of providing satisfactory predictions, covering the entire range of the simulated conditions.

In the second branch, a complete or “direct” numerical simulation of the complex spatial and temporal evolution of the interface between the two phases is followed. The most widely used methods in this direction are Marker and Cell (MAC) method, the Front Tracking (FT) method, the Arbitrary Lagrangian-Eulerian (ALE) method, the Volume-of-Fluid (VOF) method and the Level-Set (LS) method.

The VOF method can be considered as the most popular interface capturing approach and it has been also used so far, for the simulation of boiling flows. Welch and Wilson (2000) implemented a phase change model in a VOF method and simulated 1D test cases and film boiling. Welch and Rachidi (2002) extended the model by the transient heat conduction in the solid wall and simulated film boiling. Aus der Wiesche (2005) used the VOF method to simulate nucleate pool boiling of water. Hardt and Wondra (2008) have proposed a method for implementing phase change in a VOF or LS approach and performed simulations of film boiling and droplet evaporation, using a VOF method. Kunugi et al. (2002) conducted the sub-cooled pool and flow-boiling problem by MARS code and Ose and Kunugi (2011a, 2011b) conducted sub-cooled pool boiling simulations and validated the numerical results by their own visualization experimental data. Some more recent works on boiling simulation based on the VOF methods have also been reported (e.g. Pan et al., 2012; Jeon et al., 2013). However, none of the aforementioned models based on the VOF method, include any sub-model for evaporation at the 3-phase contact line. In this sense, Kunkelmann et al. (2012) implemented such a sub-model in the VOF solver of the open-source CFD package OpenFOAM (Kunkelmann and Stephan, 2009) that solves incompressible two-phase flow problems. Detailed information on the proposed numerical method can be found in Kunkelmann (2011). Already in the late 1990s, Son and Dhir (1998) numerically investigated film boiling and then Son et al. (1999) investigated the heat transfer associated with a single bubble during nucleate pool boiling, by application of the LS method. In the same decade, a lot of works have also been conducted by Dhir and co-workers for a variety of boiling flows, summarized in Dhir et al. (2001). A considerable number of more recent works on boiling heat transfer have also been published that utilize the LS method for boiling heat transfer numerical investigations (e.g. Lee and Son, 2012). The advantages of the VOF and LS methods have in many cases been combined in order to be applied for the simulation of boiling heat transfer related problems. This combined method is known as CLSVOF (Combined Level Set and Volume Of Fluid). For example, Shu (2009) in his PhD

thesis, applied the CLSVOF method to simulate boiling heat transfer using the open-source CFD package OpenFOAM, performing 2D simulations, stating that the extension of the model to 3D simulations was straightforward. Apart from the aforementioned methods, other different approaches like the Lattice Boltzmann method (Hazi and Markus, 2009) and the Phase Field method (e.g. Badillo, 2012) have been also applied for the simulation of boiling heat transfer.

In the present investigation the improved VOF-based numerical model that was presented, validated and applied to the investigation of adiabatic bubble dynamics in a previous, recent work by the authors (Georgoulas et al. 2015), is further extended for the simulation of diabatic, liquid-vapor flows with phase change. In more detail, an energy transport equation and the phase change model, originally proposed by Hardt and Wondra (2008), are implemented to a previously improved and validated (against experimental data) adiabatic, VOF solver of OpenFOAM (Georgoulas et al., 2015). The proposed phase change model (Hardt and Wondra, 2008) has been also utilized in previous similar investigations (e.g. Kunkelmann and Stephan, 2009; Kunkelmann, 2011; Magnini and Pulvirenti, 2011). The model is initially verified against an analytical solution for a bubble evaporating in a superheated liquid, for three different working fluids, with a very good degree of convergence. Apart from this, the predictions of the proposed model regarding the bubble detachment diameter and time are also validated against literature available experimental results of pool boiling of refrigerants (Lee et al., 2003). Then, the validated and optimised version of the model is further applied for the conduction of a wide range of parametric numerical simulations, identifying the effects on the bubble detachment characteristics of the initial thermal boundary layer thickness, the surface wettability, as well as the plate superheat.

NUMERICAL METHOD

Governing Equations

In this sub-section, the governing equations for mass, momentum, energy, and volume fraction are presented. It should be mentioned that liquid and vapor phases are both treated as incompressible, Newtonian fluids. The mass conservation equation is given as:

$$\nabla \cdot (\rho \vec{U}) = \dot{\rho} \quad (1)$$

where U is the fluid velocity and ρ is the bulk density. The source term on the right hand side accounts for the phase change. It should be mentioned that despite of the local source terms the mass is globally conserved since all of the mass that is removed from the liquid side of the interface is added on the vapor side. The conservation of momentum is given by the following equation:

$$\frac{\partial \rho \vec{U}}{\partial t} + \nabla \cdot (\vec{U} \cdot \rho \vec{U}) = -\nabla p + \nabla \cdot (\mu \nabla \vec{U}) + \vec{f}_{ST} + \vec{f}_g \quad (2)$$

The momentum source terms in the right hand side of the equation account for the effects of surface tension and gravity, respectively. The surface tension term is modeled according to the approach of Brackbill et al. (1992). The conservation of energy balance is given by the following equation:

$$\frac{\partial \rho c_p T}{\partial t} + \nabla \cdot (\vec{u} \cdot \rho c_p T) = \nabla \cdot (\lambda \nabla T) + \dot{h} \quad (3)$$

where, c_p is the bulk heat capacity, T the temperature field, and λ is the bulk thermal conductivity. The source term on the right hand side of the equation represents the latent heat of evaporation. The volume fraction α is advected by the flow field by the following equation:

$$\frac{\partial \alpha}{\partial t} + \nabla \cdot (\vec{u} \alpha) = \frac{\dot{\rho}}{\rho} \alpha \quad (4)$$

The source term on the right hand side of the equation is needed because, due to the local mass source terms, the velocity field is not free of divergence. It should be mentioned that the VOF method in OpenFOAM does not solve Eq. (4) implicitly, but instead applying a multidimensional universal limiter with an explicit solution algorithm (MULES). Together with the artificial interface compression algorithm (Georgoulas et al, 2015), this method ensures a sharp interface and bounds the volume fraction values between 0 and 1. Finally, the bulk fluid properties γ are computed as the averages over the two phases, weighted with the volume fraction α :

$$\gamma = \alpha \cdot \gamma_l + (1 - \alpha) \cdot \gamma_v \quad (5)$$

Phase Change Model

The phase change will be described briefly in this sub-section. Further details can be found in the work of Hardt and Wondra (2008). The evaporating mass flux at the liquid–vapor interface j_{evap} is calculated from the following relationship:

$$j_{evap} = \frac{T_{int} - T_{sat}}{R_{int} h_{lv}} \quad (6)$$

where T_{int} is the temperature of the interface, T_{sat} is the saturation temperature, R_{int} is the interfacial heat resistance and h_{lv} is the latent heat of evaporation. The interfacial heat resistance is calculated by the following relationship based in the work of Schrage (1953):

$$R_{int} = \frac{2 - a}{2a} \frac{\sqrt{2\pi R_{gas} T_{sat}^{3/2}}}{h_v^2 \rho_v} \quad (7)$$

For the cases that will be presented here, the constant α is taken equal to unity from the literature (Kunkelmann, 2011; Magnini 2012). R_{gas} is the specific gas constant of the working fluid that is calculated from the universal gas constant and the molecular weight of the working fluid.

VALIDATION OF NUMERICAL METHOD

Growth of a Spherical Bubble in a Superheated Liquid Domain

The test case that was chosen in order to validate the utilized numerical model, is the growth of a spherical bubble in an infinitely extended superheated liquid domain. More details regarding the proposed physical phenomenon are described in detail, in the work of Plesset and Zwick (1954). An analytical solution for this physical problem has been derived by Scriven (1959). According to this analytical solution the evaporating bubble radius as a function of time is given by the following relationship:

$$R(t) = 2\beta\sqrt{\gamma t} \quad (8)$$

where β is a growth constant details of which can be found in the work of Scriven (1959) and γ is the thermal diffusivity of the liquid. 2D axisymmetric simulations were performed for three different cases, Water and FC-72 liquid at equilibrium (saturation point) with their corresponding vapour phases, at a pressure value of 1013 mbar, as well as R134a liquid at equilibrium with its vapour phase at a pressure value of 840 mbar. Uniform hexahedral grids of 1 μm cell dimension were used in all cases. In Figure 1 a comparison of the numerical predictions with the analytical solution is conducted for all fluid cases. As it can be observed the numerical model adequately predicts the vapor bubble growth within the superheated liquid domain, for all the considered fluid cases.

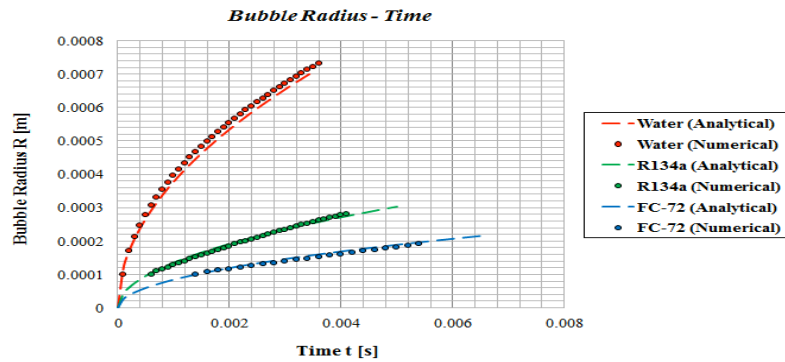


Fig. 1 Bubble radius with respect to time for all three fluid cases. Comparison of numerical (present investigation) and analytical predictions (Scriven, 1959).

Single Bubble Growth and Detachment During Pool boiling

In order to further validate the numerical model, the experiments on single bubble growth in saturated conditions on a constant wall temperature boundary condition, reported in the work of Lee et al. (2003), were selected among others, since many necessary information for their numerical reproduction are reported by the authors. In more detail, in the proposed work nucleate pool boiling experiments with constant wall temperatures were performed using R11 and R113 refrigerants, for various saturated pool boiling conditions. Here, one specific experimental run for R113 is reproduced numerically, as a validation case.

Since, the process of bubble growth and detachment in the proposed experiment can be considered to be axisymmetric, an axisymmetric computational domain was constructed for its numerical reproduction. A wedge-type computational geometry was constructed, representing a 5° section of the corresponding 3D domain in the considered physical problem. A non-uniform structured computational mesh with local refinement was used consisting of 400,000 hexahedral cells. A minimum cell size of $2\mu\text{m}$ and a maximum cell size of $4\mu\text{m}$ were selected in the bottom left and top right corners of the computational domain respectively, in order for the solution to be mesh-independent. The overall domain size in the XY plane was $2.5\text{ mm} \times 4\text{ mm}$. These dimensions were indicated from initial, trial simulations that were conducted in order to determine the minimum distances between the axis of symmetry and the side wall boundary (domain width) as well as between the bottom wall and the outlet (domain height), in order to avoid any influence of these boundaries in the computed bubble growth and detachment process.

At the solid walls, a no-slip velocity boundary condition was used with a fixed flux pressure boundary condition for the pressure values. At the lower wall, a constant contact angle of $\theta=30^\circ$ is imposed for the volume fraction field. According to Lee et al. (2003), the static contact angle of the micro-scale heater array surface was 11.4° for R113. However, the dynamic characteristics of a boiling bubble are supposed to be different with respect to the static contact angle, which is usually measured with the sessile drop method, at ambient temperature and pressure conditions. Therefore, the value of $\theta=30^\circ$ that was adopted for the proposed numerical simulation, was chosen after a series of parametric numerical simulations, where contact angles ranging from 11.4° to 60° were tested. The adopted value of $\theta=30^\circ$ indicated closest numerical predictions to the corresponding experimental observations. To notice is that when a liquid interface is moving on a surface the dynamical contact angle is always higher than the quasi-static advancing contact angle, therefore a value of the apparent contact angle higher than 11.4° is expected.

For the sidewall, a zero gradient boundary condition was used for the volume fraction values. As for the temperature field, a constant temperature of $T= 334.15\text{ K}$ (in accordance to the selected experimental run) was imposed in the bottom wall and a zero gradient boundary condition was used for the sidewall. At the outlet, a fixed-valued pressure boundary condition and a zero-gradient boundary condition for the volume fraction were used, while for the velocity values a special (combined) type of boundary condition was used that applies a zero-gradient when the fluid mixture exits the computational domain and a fixed value condition to the tangential velocity component, in cases that fluid enters the domain. Finally, a zero gradient boundary condition for the temperature field was also prescribed at the outlet boundary.

The fluid properties, the initial conditions as well as some computational details for the simulation imitating the selected experimental run are summarized in Table 1.

Table 1 Fluid properties and initial conditions.

		Density (kg/m^3)	Specific heat capacity (J/kg K)	Thermal conductivity (W/m K)	Kinematic viscosity (m^2/s)	Surface tension (N/m)	Enthalpy of vapor. (J/kg)
Phase properties (R113 at 1bar) Ts _{sat} = 320.65 K	Liquid	1508.4	940.3	0.064	3.25×10^{-7}	0.015	144350
	Vapor	7.4	691.3	0.0095	1.39×10^{-6}		
Initial Conditions	Initial bubble (seed) radius (μm)	50	Wall superheat (K)	13.5	Domain size (mm)	2.5x4.0	
			Contact angle ($^\circ$)	30			
	ITBL thickness (μm)	352	Simulation Type	Axisymm.	No. of cells		

The initial temperature of the water in the domain is assumed to be just at saturation temperature. Then a single-phase transient solution is started for a certain time period in order for the initial temperature boundary layer to be developed in the vicinity of the heated wall. After the development of the desired temperature boundary layer thickness, an initial seed bubble of 50 μm in radius is patched at the bottom wall, which immediately starts to evaporate. At this point it should be mentioned that since the initial thermal boundary layer thickness was not measured in the experiments of Lee et al. (2003), a series of parametric numerical simulations was performed, utilizing a number of successive thicknesses, developed through single-phase, natural convection at successive time instances. A thickness of 352 μm , which corresponds to a development time of 0.08 s, showed the best match with the corresponding experimental results.

In Figure 2, the reconstructed 3D evolution of the 0.5 Volume Fraction contour (interface) from the axisymmetric simulation, is compared with the corresponding experimental snapshots, for approximately the same time instances that correspond to the bubble detachment stage, while in Table 2 the numerically predicted bubble detachment characteristics, are compared with the corresponding experimental values.

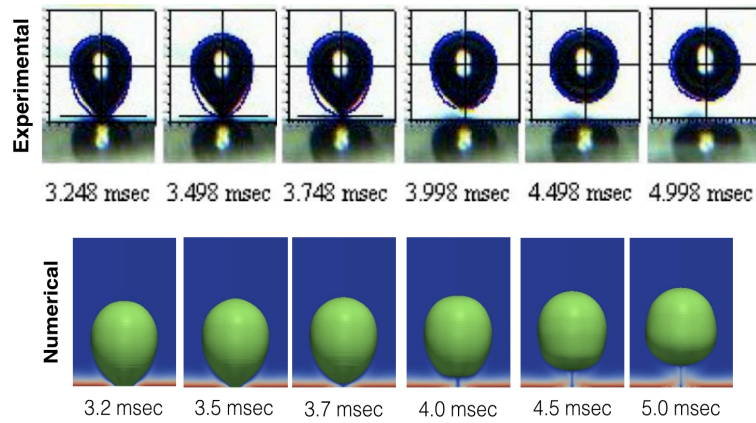


Fig. 2 Qualitative comparison of experimental (Lee et al., 2003) and numerical (present investigation) 3D bubble evolution.

Table 2 Predicted (present investigation) and measured (Lee et al., 2003), bubble detachment characteristics.

	Bubble detachment time (msec)	Equivalent bubble detachment diameter (mm)
Experimental (Lee et al., 2003)	3.748	0.704
Numerical (present investigation)	3.700	0.740
% Error	1.28	5.11

As it can be observed the numerical model predictions are in very good agreement with the corresponding experimental data. The numerically predicted spatial and temporal evolution of the generated bubble matches very well with the corresponding experimental images (Figure 2). Some small deviations in the shape of the bubble, especially after its detachment from the heated plate, can be attributed to the fact that the proposed experimental images were recorded after a few bubble cycles, while the numerical simulation images represent the first bubble cycle. However, as it is indicated in Table 2, the numerical model predictions regarding the bubble detachment time and the equivalent bubble detachment diameter, are in very close agreement with the corresponding experimental values.

PARAMETRIC NUMERICAL SIMULATIONS

In the current section of the present paper, the previously validated numerical model is further applied for the conduction of three additional series of parametric numerical simulations, aiming to identify and quantify the effects of fundamental controlling parameters in the bubble growth and detachment characteristics that were identified as being important, during the validation process that was presented and discussed previously. In more detail, the first series (Series-A) aims to identify the effect of the Initial Thermal Boundary Layer (ITBL), the second (Series-B) the effect of the triple contact line angle (wettability) and the third (Series-C) the effect of wall superheat, in the bubble growth and detachment characteristics. In all of these simulations, the same

computational domain, mesh and boundary conditions with the validation case presented in the previous section are used. The fluid properties and initial conditions for the base case, which is common to all three series, are summarized in Table 3.

Table 3 Fluid properties and initial conditions (base case).

		Density (kg/m ³)	Specific heat capacity (J/kg K)	Thermal conductivity (W/m K)	Kinematic viscosity (m ² /s)	Surface tension (N/m)	Enthalpy of vapor (J/kg)
Properties (R113 at 1bar) T _{sat} = 320.65 K	Liquid	1508.4	940.3	0.064	3.25x10 ⁻⁷	0.015	144350
	Vapor	7.4	691.3	0.0095	1.39 x10 ⁻⁶		
Initial Conditions	Initial bubble (seed) radius (μm)	50	Wall superheat (K)	13.5	Domain size (mm)	2.5x4.0	
			Contact angle (°)	11.4 – liquid side			
	ITBL thickness (μm)	352	Simulation Type	Axisymmetric	No. of cells	400000	

Effect of the initial thermal boundary layer

Since the superheated bulk liquid thermal boundary layer thickness, determines how much heat is stored in the fluid layer in the vicinity of the heated plate, it was deemed appropriate for a parametric study to be conducted, aiming to identify the effect of the ITBL thickness, on the bubble growth and detachment process. Therefore, in the current sub-section of the present paper the effect of the ITBL on the bubble detachment characteristics, is investigated numerically. For this purpose, the base case of Table 3 is utilized and additional simulations are performed by systematically varying the ITBL that is imposed in the vicinity of the heated plate (bottom wall boundary of the computational domain). In more detail, a single-phase transient simulation is first performed and the developed thermal boundary layers are extracted in certain, successive time steps. These are then used as the initial condition for the temperature field in the two-phase numerical simulations that comprise the proposed parametric analysis (Series-A numerical simulations). All the other simulation parameters are kept constant with respect to the base simulation case (Table 3). In more detail the proposed series of parametric numerical simulations (Series-A) consists of 10 different runs, A1 to A10 (with A6 being the base case of Table 3), where the ITBL thickness is varied from 136 to 680 μm, respectively. The spatial evolution of the generated bubbles for each of these cases, at the time of detachment is depicted in Figure 3.

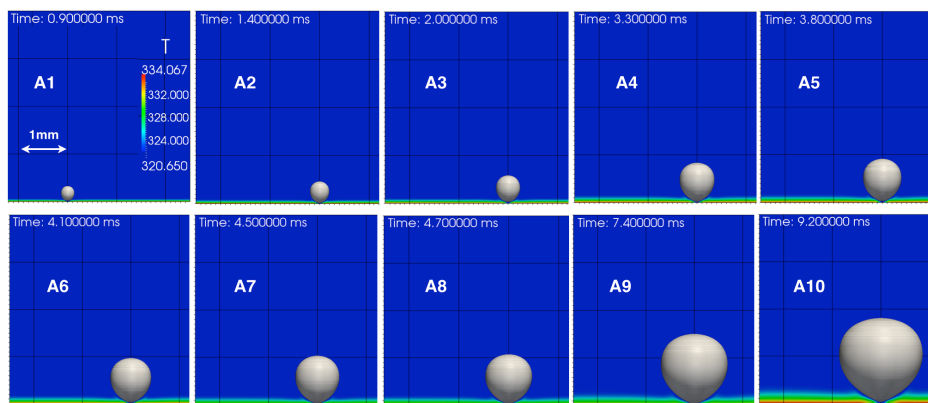


Fig. 3 Spatial evolution of generated bubble at the time of detachment for each case of Series –A parametric numerical simulations.

As it can be observed, there is a substantial increase in the bubble growth and detachment characteristics with respect to the corresponding increase in the thickness of the ITBL. The thicker the ITBL, the faster the bubble grows. A large ITBL implies that a larger amount of heat is stored in the background bulk liquid surrounding the bubble. These findings are in direct qualitative agreement with previous similar investigations (e.g. Liao et al., 2004).

But in order to quantify the exact influence of the ITBL thickness on the bubble detachment characteristics, the diagrams of Figure 4 are plotted. In more detail, the bubble detachment time with respect to the ITBL thickness is plotted in Figure 4a, while the equivalent bubble detachment diameter with respect to the ITBL thickness is plotted in Figure 4b.

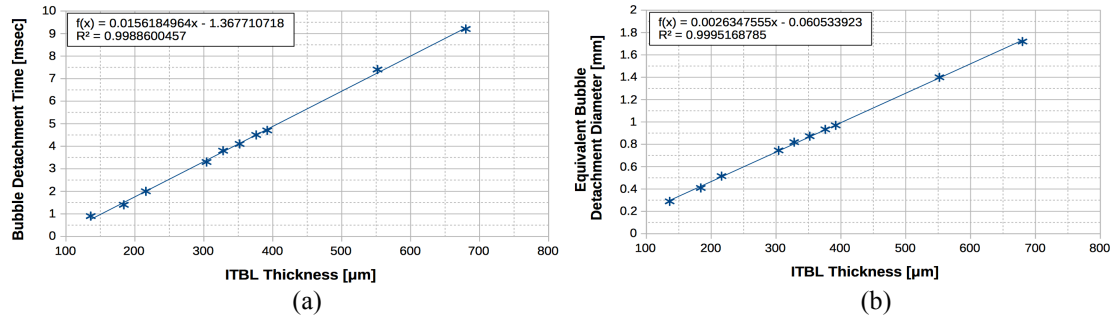


Fig. 4 Effect of ITBL thickness on (a) the bubble detachment time and (b) the equivalent bubble detachment diameter.

As it can be observed, the increase of the ITBL causes a linear increase in both the bubble detachment time as well as the equivalent bubble detachment diameter. It is characteristic that an increase of the ITBL by a factor of 5 causes a corresponding increase in the bubble detachment time and the equivalent bubble detachment diameter by a factor of 9 and 6, respectively. From all the above, it is evident that the ITBL is a very influential and important parameter in the bubble growth and detachment process at the start-up of the boiling process. Therefore, it is strongly suggested either that the bulk liquid thermal boundary layer thickness should be measured and reported in experimental studies or that enough time is left for a quasi-steady state, dynamical thermal boundary layer to develop.

Effect of the surface wettability

Past studies have identified surface wettability as one of the most important factors affecting bubble nucleation and growth dynamics. The studies of Dhir (Dhir, 2001; Dhir, 2006) provide a good summary of the current understanding. Recently it was proven that the effect of the wettability can be very strong for superhydrophobic surfaces, even generating a quasi-Leidenfrost condition at very low heat fluxes (Bourdon, 2015, Malavasi, 2015). The effect of surface wettability on bubble growth can be incorporated in a numerical model by the imposed contact angle between the vapour/liquid interface and the heated solid surface. In the current sub-section of the present paper the effect of wettability on the bubble detachment characteristics, is investigated numerically. For this purpose, the base case of Table 3 is utilized and additional simulations are performed (Series-B numerical simulations) by systematically varying the value of the contact angle on the heated plate (bottom wall boundary of the computational domain). All the other simulation parameters are kept constant with respect to the base simulation case (Table 3). A total number of 15 simulations are performed, B1 to B15 (with B1 being the base case of Table 3), varying the imposed contact angle at the bottom wall boundary from 11.4° up to 80° , by 5° increments. The spatial evolution of the generated bubbles for each of the above cases, at the time of detachment, is depicted in Figure 5. As it can be observed, initially the successive increase of the imposed contact angle from 11.4° (base case B1) up to 45° (case B8) has a minimal effect in the bubble detachment characteristics. In more detail, the bubble detachment volume slightly decreases (cases B2 and B3) and then remains almost constant (cases B4-B8). However, a slightly different effect can be observed in the predicted bubble detachment times. The bubble detachment time initially decreases (cases B2 and B3), and then it remains almost constant (cases B4-B6) and finally successively starts to increase again (cases B7 and B8). When the imposed contact angle successively increases above 45° (cases B9-B15), it causes a subsequent and considerable in each case increase in the bubble detachment volume. Approximately the same trend can be observed also in the bubble detachment time. However, it is characteristic that while the bubble detachment time continuously increases with the corresponding increase in the contact angle (cases B9-B12) at a certain point (cases B13 and B14) remains almost constant and then continue to increase (case B15). Another interesting observation is the fact that for contact angles greater than 70° (cases B14 and B15), the bubble departs from the surface leaving behind a small residual bubble nucleus on the surface.

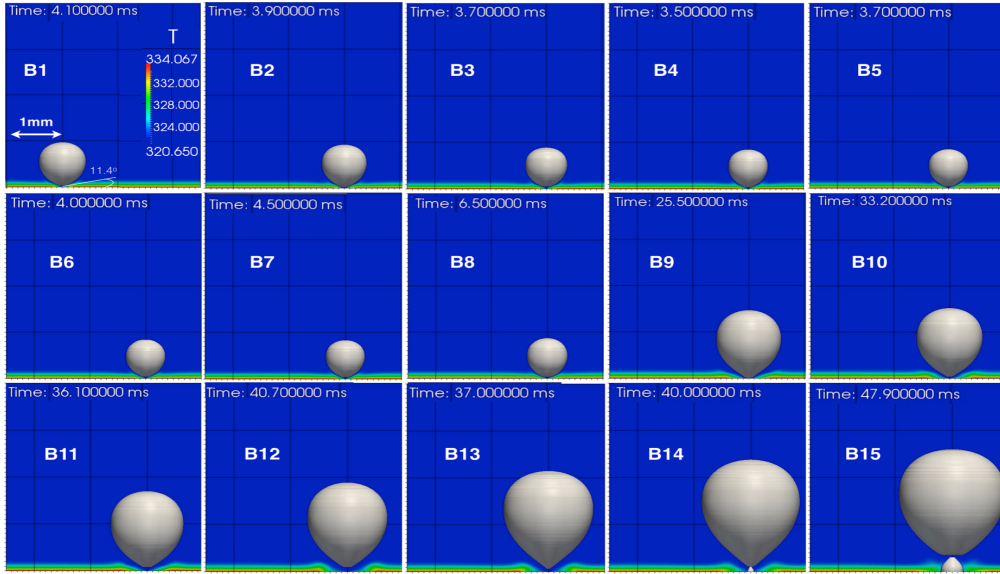


Fig. 5 Spatial evolution of generated bubble at the time of detachment for each case of Series –B parametric numerical simulations.

A more quantitative illustration of all the above-mentioned observations can be depicted in the diagrams of Figure 6, where the bubble detachment time (Figure 6a) and the equivalent bubble detachment diameter (Figure 6b) are plotted with respect to the imposed contact angle at the heated wall.

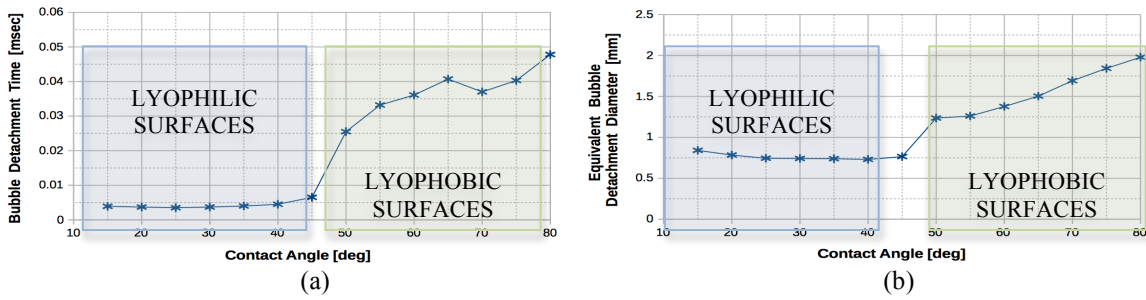


Fig. 6 Effect of contact angle on (a) the bubble detachment time and (b) the equivalent bubble detachment diameter.

It is important to note that increasing the contact angle by an approximate factor of 8 causes a significant increase in the bubble detachment time by a factor of 10, while the equivalent bubble detachment diameter increases by a smaller but still significant factor of 2.7.

As it can also be confirmed by the diagrams of Figure 6, the bubble detachment characteristics seem to be almost unaffected by contact angles lower than 45° showing an irregular increase for contact angles greater than this limiting value. This is very important since it leads to the identification of two regimes, one linked to lyophobic surfaces, where the influence of the wettability is important and leads to an increase of the detachment time and volume, and another regime for lyophilic surfaces where the wettability effect is minor. There is also a transition region for a contact angle value of about 45° . This transition angle should be a function of the liquid properties, being easily depended on the liquid-vapour density differences for example.

Effect of the wall superheat

In the current sub-section of the present paper, the effect of wall superheat on the bubble detachment characteristics is also investigated numerically. It is well known that this parameter is very important for the pool boiling process, but here it is intended to have an estimate of the effect for R113 for future experimental comparisons. For this purpose, the base case of Table 3 is again utilized and additional simulations are performed (Series-C numerical simulations) by systematically varying the value of the heated plate superheat (bottom wall boundary of the computational domain). All the other simulation parameters are kept constant with respect to the base simulation case (Table 3). As it can be seen, a total of 9 simulations are performed, C1 to C9

(with C3 being the base case of Table 3), varying the bottom wall superheat from 5.5 K up to 19.5 K. It should be mentioned that, a single-phase transient numerical simulation is initially performed in each of the above cases and the developed ITBL at 0.08s is used as the initial condition for the temperature field in the two-phase simulations. This is done in order to start in each case with approximately the same thickness of the ITBL but with a different superheat. The spatial evolution of the generated bubbles for each of the above cases, at the time of detachment, is depicted in Figure 7.

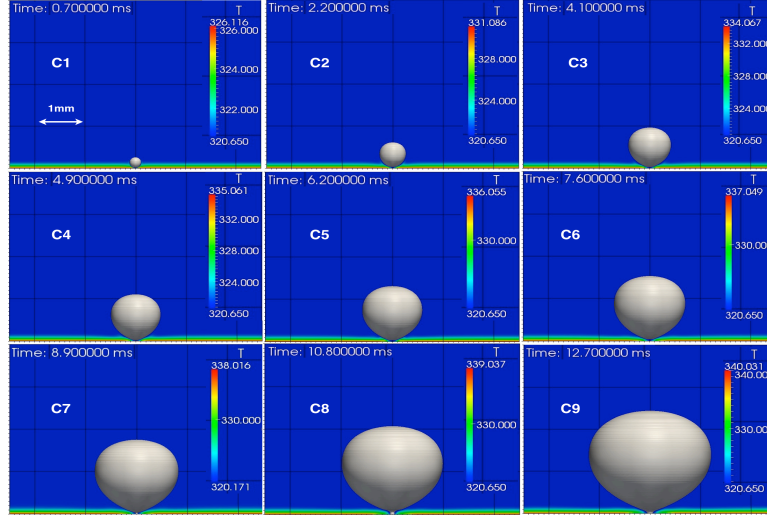


Fig. 7 Spatial evolution of generated bubble at the time of detachment for each case of Series -C parametric numerical simulations.

As it can be observed both the bubble detachment time as well as the bubble detachment volume are highly sensitive to the wall superheat. In more detail, a successive increase in the bottom wall superheat causes a quite considerable, subsequent increase in the bubble detachment characteristics. In more detail, the higher the wall superheat, the faster the bubble grows. But in order to quantify the exact influence of the wall superheat on the bubble detachment characteristics, the diagrams of Figure 8 are plotted. In more detail, the bubble detachment time with respect to the applied wall superheat is plotted in Figure 8a, while the equivalent bubble detachment diameter with respect to the applied wall superheat is plotted in Figure 8b.

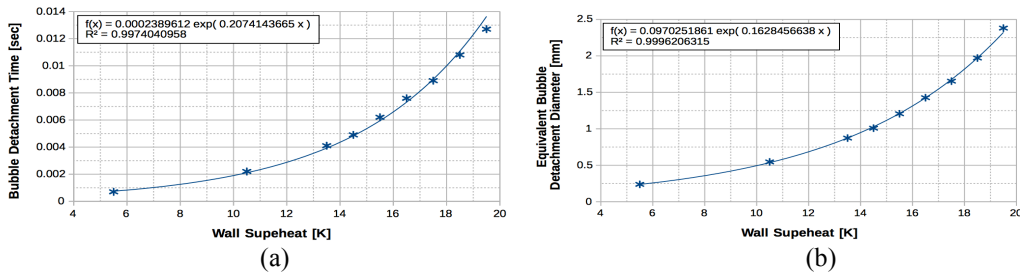


Fig. 8 Effect of wall superheat on (a) the bubble detachment time and (b) the equivalent bubble detachment diameter.

As it can be observed the increase of the applied wall superheat causes an exponential increase in both the bubble detachment time as well as the equivalent bubble detachment diameter. It is characteristic that an increase in the applied superheat by a factor of just 3.5, causes a corresponding increase in the bubble detachment time and the equivalent bubble detachment diameter by an approximate factor of 18 and 10, respectively. These findings and observations are in direct qualitative agreement with previous similar investigations (e.g. Sanna, 2010).

CONCLUSIONS

In the present paper, heat transfer and phase-change are coupled with a previously improved and validated, by the authors, Volume Of Fluid (VOF) model for adiabatic bubble dynamics (Georgoulas et al., 2015) within the OpenFOAM CFD framework. The model is initially tested against the predictions of an existing analytical

solution for cases of evaporating bubble growth in a superheated liquid domain. Moreover, the predictions of the proposed model regarding the bubble detachment characteristics are also validated against literature available experimental data on saturated pool boiling of refrigerants. From the overall comparison of the numerical predictions with the aforementioned analytical solution as well as with the previously published experimental measurements, it is concluded that the proposed VOF-based numerical model, can successfully capture the bubble growth and/or detachment characteristics due to evaporation in a superheated liquid domain or during saturated pool boiling due to the presence of a superheated plate.

From the further application of the validated and optimized version of the model to a wide range of parametric numerical simulations, it is found that the bubble growth and detachment characteristics are highly sensitive to the initially developed thermal boundary layer thickness, following a linear relationship. The systematic variation of the imposed contact angle (heated surface wettability), lead to the identification of a threshold value below which, the effect on the bubble detachment characteristics is minimal while above this value the influence is quite significant. Finally, the bubble detachment characteristics follow an exponential increase with the corresponding increase in the superheat of the heated plate.

Summarising, the present investigation adds significantly to the existing knowledge on saturated pool boiling, since a diabatic, VOF-based, CFD model that takes into consideration phase change due to evaporation is comprehensively validated against literature available analytical solutions and experimental measurements, and then further applied for the examination of the effect of fundamental controlling parameters on the bubble growth process, identifying their exact quantitative influence on the bubble detachment diameter and time, indicating at the same time their relative importance.

Finally, it can be said that the use of the enhanced VOF-based interface capturing approach that is presented, validated and applied in the present investigation, constitutes a quite promising tool for the simulation of a wide range of phase-change phenomena.

ACKNOWLEDGMENTS

The results presented in the present paper, constitute part of a more wider research work, which is related to the development of a VOF-based flow boiling model, able to predict the bubble detachment characteristics in cases of diesel fuel flow boiling within injector nozzles, and it has received funding from the People Programme (IAPP Marie Curie Actions) of the European Union's Seventh Framework Programme FP7/2007-2013/under REA grant agreement no. 324313. The authors would also like to acknowledge the contribution of the super-computing facilities of CINECA, in Bologna (Italy).

REFERENCES

- Badillo, A., 2012, Quantitative phase-field modeling for boiling phenomena. *Physical Review E*, Vol. 86, pp. 041603.
- Brackbill, J.U., Kothe, D.B., and Zemach, 1992, A continuum method for modeling surface tension, *Journal of Computational Physics*, Vol. 100 (2), pp. 335-354.
- Schrage, R.W., 1953, A theoretical study of interphase mass transfer. *Columbia University Press, New York*, pp. 32-43.
- B. Bourdon, E. Bertrand, P. Di Marco, M. Marengo, R. Rioboo, J. de Coninck, 2015, Wettability influence on the onset temperature of pool boiling: experimental evidence onto ultra-smooth surfaces, *ADVANCES IN COLLOID AND INTERFACE SCIENCE*, 221, pp. 34–40
- Cheung, S.C.P., Vahaji, S., Yeoh, G.H., and Tu J.Y., 2014, Modeling subcooled flow boiling in vertical channels at low pressures – Part 1: assessment of empirical correlations, *International Journal of Heat and Mass Transfer*, Vol. 75, pp. 736-753.
- Der Wiesche S.A., 2005, Bubble growth and departure during nucleate boiling: the occurrence of heat flux reversal, *Proc. of the 4th International Conference on Computational Heat and Mass Transfer*.
- Dhir. V. K., 2001, Numerical simulations of pool-boiling heat transfer, *AIChE Journal*, Vol. 47, pp. 813-834.
- Dhir, V. K., 2006, Mechanistic Prediction of Nucleate Boiling Heat Transfer Achievable or a Hopeless Task?, *ASME J. Heat Transfer*, Vol. 128 (1), pp. 1–12.
- Georgoulas A., Koukouvini, P., Gavaises, M., and Marengo M., 2015, Numerical investigation of quasi-static bubble growth and detachment from submerged orifices in isothermal liquid pools: The effect of varying fluid properties and gravity levels, *International Journal of Multiphase Flows*, Vol. 74, pp. 59–78.
- Hardt, S., and Wondra, F., 2008, Evaporation model for interfacial flows based on a continuum-field representation of the source terms, *Journal of Computational Physics*, Vol. 227, pp. 5871-5895.
- Hazi, G., Markus, A., 2009, On the bubble departure diameter and release frequency based on numerical simulation results, *International Journal of Heat and Mass Transfer*, Vol. 52, pp.1472-1480.

- Jeon, S.S., Kim, S.S., and Park, G.C., 2011, Numerical study of condensing bubble in subcooled boiling flow using volume of fluid model. *Chemical Engineering Science*, Vol. 66, pp. 5899-.
- Krepper, E., Rzehak, R., Lifante, C., and Frank, T., 2013, CFD for subcooled flow boiling: coupling wall boiling and population balance models, *Nuclear Engineering and Design*, Vol. 255, pp. 330-346.
- Kunkelmann, C., Ibrahim, K., Schweizer, N., Herbert, S., Stephan, P., and Gambaryan-Roisman T., 2012, The effect of three-phase contact line speed on local evaporative heat transfer: experimental and numerical investigations, *International Journal of Heat and Mass Transfer*, Vol. 55, pp. 1896-.
- Kunkelmann, C., and Stephan, P., 2009, CFD simulation of boiling flows using Volume-of-Fluid method within OPENFOAM, *Numerical Heat Transfer A*, Vol. 56, pp. 631-.
- Kunkelmann C., 2011, Numerical Modeling and Investigation of Boiling Phenomena, *PhD Thesis, Technische Universität Darmstadt*.
- Kunugi, T., Saito, N., Fujita, Y., and Serizawa, A., 2002, Direct numerical simulation of pool and forced convective flow boiling phenomena, *Heat Transfer*, Vol. 3, pp. 497-.
- Kurul, N., and Podowski, M.Z., 1990, Multidimensional effects in forced convection subcooled boiling, Proc. of the 9th International Heat Transfer Conference, Jerusalem, Israel (1990).
- Lee H. C., Oh B. D., Bae S. W., and Kim M. H., 2003, Single bubble growth in saturated pool boiling on a constant wall temperature surface, *International Journal of Multiphase Flow*, Vol. 29, pp.1857–1874.
- Lee, W., and Son. G., 2012, Numerical study of bubble growth and boiling heat transfer on a microfinned surface, *International Communications in Heat and Mass Transfer*, Vol. 39, pp. 52-.
- Liao J., Mei R., and Klausner J. F., 2004, The influence of the bulk liquid thermal boundary layer on saturated nucleate boiling, *International Journal of Heat and Fluid Flow*, Vol. 25, pp.196–208.
- Lopez-de-Bertodano, M.A., and Prabhudharwadkar, D., 2010, CFD Two Fluid Model for Adiabatic and Boiling Bubbly Flows in Ducts, *Computational Fluid Dynamics*, eds. O.H. Hyung Woo, INTECH, Croatia, ISBN 978-953-7619-59-6, pp. 420.
- Magnini, M., and Pulvirenti. B., 2011, Height Function interface reconstruction algorithm for the simulation of boiling flows, *Proc. of the 6th International Conference on Computational and Experimental Methods in Multiphase and Complex Flows, Kos, Greece*.
- Magnini, M., 2012, CFD modelling of two-phase boiling flows in the slug flow regime with an interface capturing technique, *PhD Thesis, University of Bologna*.
- Malavasi I., B. Bourdon, P. Di Marco, J. de Coninck, M. Marengo, 2015, Appearance of a low superheat “quasi-Leidenfrost” regime for boiling on superhydrophobic surfaces, *INTERNATIONAL COMMUNICATIONS IN HEAT AND MASS TRANSFER*, 63, pp. 1–7.
- Ose Y., and Kunugi, T., 2011a, Numerical Study on Subcooled Pool Boiling, *Progress in Nuclear science and Technology*, Vol. 2, pp.125-.
- Ose, Y., and Kunugi, T., 2011b, Development of a Boiling and Condensation Model on Subcooled Boiling Phenomena, *Energy Procedia*, Vol. 9, pp. 605-.
- Pan, L.M., Tan, Z.W., Chen, D.Q., and Xue L.C., 2012, Numerical investigation of vapor bubble condensation characteristics of subcooled flow boiling in vertical rectangular channel. *Nuclear Engineering Design*, Vol. 248, pp. 126-.
- Plesset, M.S., and Zwick. S.A., 1954, The growth of vapor bubbles in superheated liquids, *Journal of Applied Physics*, Vol. 25, pp. 493-500.
- Prabhudharwadkar, D., Lopez-de-Bertodano, M.A., Hibiki, T., and Buchanan, J.R., 2014, Assessment of subcooled boiling wall boundary correlations for two-fluid model CFD, *International Journal of Heat and Mass Transfer*, Vol. 79, pp. 602-617.
- Sanna A., 2010, Numerical investigation of saturated pool boiling on thin walls, *PhD Thesis, School of Engineering and Design, Brunel University*.
- Scriven, L.E., 1959, On the Dynamics of Phase Growth, *Chemical Engineering Science*, Vol. 10, pp. 1-3.
- Shu. B., 2009, Numerische Simulation des Blasensiedens mit Volume-Of-Fluid- und Level-Set-Methode, *PhD thesis, Technische Universität Darmstadt*.
- Son, G., and Dhir, V.K., 1998, Numerical simulation of film boiling near critical pressures with a level set method, *Journal of Heat Transfer*, Vol. 120, pp.183-.
- Son, G., Dhir, V. K., and Ramanujapu N., 1999, Dynamics and heat transfer associated with a single bubble during nucleate boiling on a horizontal surface, *Journal of Heat Transfer*, Vol. 121, pp. 623-.
- Welch, S.W.J., and Wilson J., 2000, A volume of fluid based method for fluid flows with phase change, *Journal of Computational Physics*, Vol. 160, pp. 662-682.
- Welch S.W.J., and Radichi, T., 2002, Numerical computation of film boiling including conjugate heat transfer, *Numerical Heat Transfer, Part. B*, Vol. 42, pp. 35-53.
- Yun, B.J., Splawski, A., Lo, S., and Song C.H., 2013, Prediction of a subcooled boiling flow with advanced two-phase flow models. *Nuclear Engineering and Design*, Vol. 255, pp. 330-346.